

## Targeted positron emission tomography imaging of CXCR4 expression in patients with acute myeloid leukemia

Peter Herhaus,<sup>1</sup> Stefan Habringer,<sup>1,2,#</sup> Kathrin Philipp-Abbrederis,<sup>1</sup> Tibor Vag,<sup>3</sup> Carlos Gerngross,<sup>3</sup> Margret Schottelius,<sup>4</sup> Julia Slotta-Huspenina,<sup>5</sup> Katja Steiger,<sup>5</sup> Torben Altmann,<sup>6</sup> Tanja Weißer,<sup>1</sup> Sabine Steidle,<sup>1</sup> Markus Schick,<sup>1</sup> Laura Jacobs,<sup>3</sup> Jolanta Slawska,<sup>3</sup> Catharina Müller-Thomas,<sup>1</sup> Mareike Verbeek,<sup>1</sup> Marion Subklewe,<sup>2,6</sup> Christian Peschel,<sup>1,2</sup> Hans-Jürgen Wester,<sup>5</sup> Markus Schwaiger,<sup>2,3</sup> Katharina Götze,<sup>1,2</sup> and Ulrich Keller<sup>1,2</sup>

<sup>1</sup>III Medical Department, Technische Universität München; <sup>2</sup>German Cancer Consortium (DKTK), German Cancer Research Center (DKFZ), Heidelberg; <sup>3</sup>Nuclear Medicine Department, Technische Universität München; <sup>4</sup>Pharmaceutical Radiochemistry, Technische Universität München; <sup>5</sup>Department of Pathology, Technische Universität München; and <sup>6</sup>III Medical Department, Ludwig-Maximilians-Universität, Munich, Germany

*#PH and SH contributed equally to this work.*

©2016 Ferrata Storti Foundation. This is an open-access paper. doi:10.3324/haematol.2016.142976

Received: January 18, 2016.

Accepted: May 4, 2016.

Pre-published: May 12, 2016.

Correspondence: [ulrich.keller@tum.de](mailto:ulrich.keller@tum.de)

---

## **Supplementary Material**

### **Targeted positron emission tomography imaging of CXCR4 expression in patients with acute myeloid leukemia**

Peter Herhaus<sup>1, #</sup>, Stefan Habringer<sup>1, 6, #</sup>, Kathrin Philipp-Abbrederis<sup>1</sup>, Tibor Vag<sup>2</sup>, Carlos Gerngross<sup>2</sup>, Margret Schottelius<sup>3</sup>, Julia Slotta-Huspenina<sup>4</sup>, Katja Steiger<sup>4</sup>, Torben Altmann<sup>5</sup>, Tanja Weißer<sup>1</sup>, Sabine Steidle<sup>1</sup>, Markus Schick<sup>1</sup>, Laura Jacobs<sup>2</sup>, Jolanta Slawska<sup>2</sup>, Catharina Müller-Thomas<sup>1</sup>, Mareike Verbeek<sup>1</sup>, Marion Subklewe<sup>5, 6</sup>, Christian Peschel<sup>1, 6</sup>, Hans-Jürgen Wester<sup>4</sup>, Markus Schwaiger<sup>2, 6</sup>, Katharina Götze<sup>1, 6</sup>, and Ulrich Keller<sup>1, 6</sup>

<sup>1</sup> III. Medical Department, Technische Universität München, Munich, Germany

<sup>2</sup> Nuclear Medicine Department, Technische Universität München, Munich, Germany

<sup>3</sup> Pharmaceutical Radiochemistry, Technische Universität München, Munich, Germany

<sup>4</sup> Department of Pathology, Technische Universität München, Munich, Germany

<sup>5</sup> III. Medical Department, Ludwig-Maximilians-Universität, Munich, Germany

<sup>6</sup> German Cancer Consortium (DKTK), German Cancer Research Center (DKFZ), Heidelberg, Germany

## **Supplementary Methods**

### **Patients**

In the CXCR4-expression cohort, sample source was either BM (59 patients) or peripheral blood (PB) (8 patients).

Ten patients with active myeloid disease underwent PET imaging for CXCR4. Detailed characteristics of the imaging cohort are shown in Table S3. PET imaging of 5 patients with non-hematologic malignancies (in detail: 2 patients with sarcoma, 1 patient with malignant melanoma, 1 patient with laryngeal squamous cell carcinoma, 1 patient with pancreatic carcinoma.) examined in a different analysis served as a control group.

The design of this study is not confirmatory. There were no pre-specified hypotheses that would have allowed for sample size calculation. It is an observational pilot study used to conduct explorative analyses. Therefore, the sample size was chosen to serve this purpose. It enabled the computation of descriptive and explorative statistics.

### **Cell lines and cell culture**

The human AML cell lines Molm-13, MV4-11, NOMO-1 and NB4 were cultured in RPMI 1640 with 20% fetal calf serum (FCS) for KG1a and 10% FCS for all other lines. OCI-AML2 and OCI-AML3 were cultured in high glucose (4.5g/l) DMEM supplemented with 10% FCS. KG1a medium with 1% non-essential amino acids and 1mM sodium pyruvate was used

for Mono-Mac-1, with 10µg/ml human insulin additionally for Mono-Mac-6. OCI-AML5 were cultured in Alpha-MEM with 20% FCS, and 10% supernatant of 5637 cells. GF-D8 were cultured in RPMI 1640 with 20% FCS and 10% supernatant of 5637 cells. Daudi cells were cultured in RPMI 1640 supplemented with 20 % FCS, 1% non-essential amino acids and 0.05mM 2-mercaptoethanol. All media were supplemented with 100 U/ml penicillin and 100µg/ml streptomycin. All cell lines were obtained from the German Collection of Microorganisms and Cell Cultures (DSMZ, Leibniz, Germany).

Cells were maintained at 37°C in a 5% CO<sub>2</sub> humidified atmosphere. All media and supplements were obtained from Gibco/Life Technologies (Carlsbad, CA, USA).

### **RNA isolation and real-time PCR**

RNA extraction was performed using the RNeasy Mini Kit (Qiagen, Venlo, Netherlands). cDNA synthesis was performed using the Omniscript RT Kit according to the manufacturer's protocol (Qiagen, Venlo, Netherlands). Real-time PCR was performed using Platinum SYBR-Green Q PCR SuperMix-UDG (Thermo Fisher Scientific, Waltham, MA, USA) on a StepOnePlus System (Applied Biosystems, Waltham, MA, USA). Data analysis was performed by comparing  $\Delta\Delta C_t$  values of AML cell lines with peripheral blood mononuclear cells (PBMCs) of 3 healthy individuals. Primer sequences are available upon request.

### **CRISPR-Cas9 mediated knock-out of CXCR4**

For construction of a lentiviral vector coding for both Cas9 and a CXCR4-specific sgRNA, we cloned single guide sequences (Supplementary Figure S3) into lentiCRISPRv2 (Addgene plasmid #52961) previously modified by inserting a ccdB suicide cassette (kindly provided by Marc Schmidt-Supprian, Munich). Guides were designed with CHOPCHOP ([chopchop.rc.fas.harvard.edu](http://chopchop.rc.fas.harvard.edu)). For stable transduction, OCI-AML3 cells were incubated with viral supernatants produced by HEK293T cells transfected with the respective lentiCRISPRv2-plasmid and psPAX2 and pMD2.G packaging plasmids (Addgene plasmid #12260 and #12259 respectively) and centrifuged for 1h at 1200rpm and 32°C twice over a period of 8h. We used 2 µg/ml puromycin to select for stable integration of lentiCRISPRv2 into OCI-AML3 cells. We sequenced the predicted cutting site in the genomic DNA by Sanger sequencing (GATC biotech, Konstanz, Germany) and assessed efficiency of indel formation by Tracking of Indels by DEcomposition (TIDE).

### **Migration assay**

Cell migration towards human CXCL12 (R&D Systems, Minneapolis, MN, USA) was performed in transwell plates with 5µm pore size (Corning Inc., Corning, NY, USA). Cells

were plated in medium without FCS with 0.5% bovine serum albumin (BSA) in the top chamber and 100ng/ml CXCL12 was added into the lower chamber. After 4h at 37°C, cells that had migrated to the lower chamber were quantified by flow cytometry using CountBright absolute counting beads (Thermo Fisher, Waltham, MA, USA).

### **Mice and tumor xenograft experiments**

Animal studies were performed in agreement with the Guide for Care and Use of Laboratory Animals published by the US National Institutes of Health (NIH Publication No. 85-23, revised 1996), in compliance with the German law on the protection of animals, and with approval of the responsible regional authorities (Regierung von Oberbayern). CB17-SCID (SCID) mice were obtained from Charles River Laboratories (Calco, Italy). For xenograft experiments, 6-8 weeks old mice were injected subcutaneously into both flanks with  $6 \times 10^6$  KG1a,  $5 \times 10^6$  OCI-AML3,  $7,5 \times 10^6$  NOMO-1,  $5 \times 10^6$  OCI-AML3 CXCR4 knock-out cells mixed with equal amounts of growth factor reduced Matrigel (Corning Inc., Corning, NY, USA) and PBS. When tumor size reached approximately 1cm, mice were subjected to PET imaging with [ $^{68}\text{Ga}$ ]Pentixafor (Scintomics, Fürstfeldbruck, Germany).

### **Blood counts and flow cytometry**

All analyses on patient derived material were performed upon signed informed consent of the patients. PB white blood cell counts, hemoglobin and platelet counts from AML patients were measured using an automated Advia 120 (Siemens, Erlangen, Germany). For flow cytometry analysis, PB and BM samples were collected in heparin tubes, filtered and subjected to erythrocyte lysis. Cell populations of interest were selected by sequential gating using Kaluza Flow Analysis Software (Beckman Coulter, Brea, CA, USA). The gating strategy is based on CD45 staining versus side-angle light scatter (SSC) properties as a primary gate to discern CD45<sup>low</sup> blasts with low SSC properties. Colored back-gating was used to ensure correct gating of all subpopulations. Cells were also stained for expression of CD34 and CD117. As not all AML samples show expression of CD34 on the blast population, CD117 was used for colored back-gating of blast cells in most samples. For statistical data analysis, median fluorescence intensity of surface CXCR4 expression was divided by median fluorescence intensity of the isotype control of the corresponding subpopulation. Details on the gating strategy are given in Supplementary Figure S1. The following antibodies were used: Beckman Coulter: CD45-ECD (clone J33), CD34-FITC (clone 581), CD117-PE (clone 104D2D1); BD Biosciences (Franklin Lakes, NJ, USA): CXCR4-PE (clone 12G5). Surface CXCR4 levels of human AML cell lines were determined by flow cytometry (Cyan ADP, Beckman Coulter) using the same CXCR4-PE and isotype control antibody as in the patient samples. Data were analyzed using FlowJo (FlowJo, Ashland, OR, USA).

### Synthesis of [<sup>68</sup>Ga]Pentixafor

Synthesis of [<sup>68</sup>Ga]Pentixafor was performed in a fully automated, GMP-compliant procedure using a GRP<sup>®</sup> module (SCINTOMICS GmbH, Fürstfeldbruck, Germany) equipped with disposable single-use cassette kits (ABX, Radeberg, Germany), using the method (1, 2) and standardized labeling sequence previously described. Prior to injection, the quality of [<sup>68</sup>Ga]Pentixafor was assessed according to the standards described in the European Pharmacopoeia for [<sup>68</sup>Ga]-Edotreotide (European Pharmacopoeia; Monograph 01/2013:2482; available at [www.edqm.eu](http://www.edqm.eu)).

### CXCR4 PET imaging of mice

PET scans of xenotransplanted AML cell lines in SCID mice were performed as previously described (3). Briefly, mice were intravenously injected with 12 MBq/mouse [<sup>68</sup>Ga]Pentixafor and static images were acquired for 15 min starting 75 min post-injection on a  $\mu$ PET-system (Inveon, Siemens, Erlangen, Germany). Voxel intensities were calculated by placing three-dimensional regions of interest within the tumors. PET scans were acquired 75 min post PET tracer injection.

### PET/MR and PET/CT imaging studies in patients

Nine of 10 [<sup>68</sup>Ga]Pentixafor scans were performed on a PET/MRI device (Siemens Biograph mMR; Siemens Medical Solutions, Germany). One of 10 [<sup>68</sup>Ga]Pentixafor scan was performed on a PET/CT device (Siemens Biograph mCT 64; Siemens Medical Solutions, Germany). Prior to [<sup>68</sup>Ga]Pentixafor PET, patients fasted at least 4 hours. Injected activities ranged from 161-340 MBq. For generation of attenuation-maps, a coronal 2-point Dixon 3D volumetric interpolated examination (VIBE) T1 weighted (T1w) MR sequence was performed as recently published (4). For diagnostic imaging, both a coronal T1 TSE (TR/TE 600/8.7, slice thickness 5 mm, matrix 384x230) and a T2w STIR (short  $\tau$  inversion recovery) sequence with fat suppression (TR/TE/TI 5000ms/56ms/220ms, slice thickness 5 mm, matrix 106x256) were acquired. PET emission data was simultaneously measured in three-dimensional mode with a 200x200 matrix with 2-3 min emission time per bed position. After decay and scatter correction, PET data was reconstructed iteratively with attenuation correction using a dedicated software (Siemens Esoft).

In one patient with extramedullary relapse, an additional [<sup>18</sup>F]FDG-PET/CT scan (Siemens Biograph mCT 64; Siemens Medical Solutions, Germany) was performed 5 days after [<sup>68</sup>Ga]Pentixafor imaging. Before image acquisition, the patient fasted for 6 hours prior to injection of a standard dose of 4.5 MBq per kg body weight. Corresponding CT low dose scans for attenuation correction were acquired using a low-dose protocol (20 mAs, 120 keV,

a 512x512 matrix, 5 mm slice thickness, increment of 30 mm/s, rotation time of 0.5 s, and pitch index of 0.8) including the base of the skull to the proximal thighs.

### **PET and MR analysis**

All MRI scans were scored by a board certified radiologist, and all PET scans were scored by a board certified nuclear medicine physician. BM infiltration on MRI was demonstrated by a diffuse decrease of the BM signal on T1w images, as described previously (5).

All PET scans were interpreted in a binary visual fashion as positive for disease or negative for disease according to the criteria previously described (6). Briefly, presence of focal areas of detectable increased tracer uptake within bones (i.e. more intense than background BM uptake excluding articular processes, with or without any underlying lesion identified by MRI) were rated as positive.

For semiquantitative analysis of tracer accumulation in the BM, SUVmax were measured in representative sites by using 2D regions of interests (ROIs) with a diameter of 1 cm. These included the 7<sup>th</sup> cervical, the 12<sup>th</sup> thoracic spine, the 5<sup>th</sup> lumbar spine and the left and right os ilium. For comparison of tracer accumulation in uninvolved BM, SUVmax measurements were additionally performed in five PET scans of patients without hematological malignancies or other osseous manifestations analogous to the measurements described above.

### **Immunohistochemistry**

Immunohistochemistry for CXCR4 expression was conducted as follows: After heat-induced antigen retrieval (10mM citrate buffer, pH6, 20 min) and protein and peroxidase blocking (Universal Block (Dako, Jena, Germany) and 3 % normal goat serum (Abcam, Cambridge, UK)), immunohistochemistry was performed with a Dako autostainer using an antibody against CXCR4 (1:30, Abcam, ab124824, clone UMB-2). Antibody detection was performed using the Dako Envision-HRP rabbit labeled polymer visualized by diaminobenzidine (DAB) (KPL, Milford, MA, USA). Counterstaining was performed with hematoxylin.

Immunohistochemistry for CD34 (1:200), CD43 (1:100) and CD117 (1:500) was performed using an automated immunostainer with the VIEW DAB detection kit (Ventana Medical System, Roche) according to the company's protocols for open procedures. Antibodies for CD34, CD117 and CD43 were used according to the manufacturer's instructions. Appropriate positive controls were used to confirm the adequacy of the staining.

### **Statistical analysis**

All statistical tests were performed using GraphPad Prism (GraphPad Software, La Jolla, CA). P-values < 0.05 were considered statistically significant. Quantitative values were expressed as mean  $\pm$  standard deviation (SD) or standard error of the mean (SEM) as indicated. Comparisons of related metric measurements were performed using Wilcoxon-signed rank test and the Mann-Whitney-U test or Student's t-test was used to compare quantitative data between two independent samples. Analysis of variance (ANOVA) statistical test was used to analyze the differences between group means. The Pearson coefficient (r) was calculated to determine correlation.

## References

1. Demmer O, Gourni E, Schumacher U, Kessler H, Wester HJ. PET Imaging of CXCR4 Receptors in Cancer by a New Optimized Ligand. *Chemmedchem*. 2011 Oct 4;6(10):1789-91.
2. Gourni E, Demmer O, Schottelius M, D'Alessandria C, Schulz S, Dijkgraaf I, et al. PET of CXCR4 expression by a (68)Ga-labeled highly specific targeted contrast agent. *Journal of nuclear medicine : official publication, Society of Nuclear Medicine*. 2011 Nov;52(11):1803-10.
3. Wester HJ, Keller U, Schottelius M, Beer A, Philipp-Abbrederis K, Hoffmann F, et al. Disclosing the CXCR4 expression in lymphoproliferative diseases by targeted molecular imaging. *Theranostics*. 2015;5(6):618-30.
4. Drzezga A, Souvatzoglou M, Eiber M, Beer AJ, Furst S, Martinez-Moller A, et al. First clinical experience with integrated whole-body PET/MR: comparison to PET/CT in patients with oncologic diagnoses. *Journal of Nuclear Medicine*. 2012 Jun;53(6):845-55.
5. Silva JR, Jr., Hayashi D, Yonenaga T, Fukuda K, Genant HK, Lin C, et al. MRI of bone marrow abnormalities in hematological malignancies. *Diagnostic and interventional radiology*. 2013 Sep-Oct;19(5):393-9.
6. Zamagni E, Patriarca F, Nanni C, Zannetti B, Englari E, Pezzi A, et al. Prognostic relevance of 18-F FDG PET/CT in newly diagnosed multiple myeloma patients treated with up-front autologous transplantation. *Blood*. 2011 Dec 1;118(23):5989-95.

## Supplementary Figure and Table Legends

### Supplementary Figure S1. Gating strategy to assess CXCR4 expression on AML blasts.

- A The gating strategy is based on CD45 staining versus side-angle light scatter (SSC) properties as a primary gate to discern CD45<sup>low</sup> blasts with low SSC properties. CD117 was used for colored back-gating to ensure correct gating of all subpopulations.
- B In selected patients intraindividual comparison of AML blast CXCR4 positivity was performed by comparing expression with lymphocytes using the lymphocyte gate shown in (a). Representative dot blot analyses are shown.

### Supplementary Figure S2. No significant correlation between blast CXCR4 expression and disease/patient characteristics.

- A-F CXCR4 blast expression in the patient cohort described in Supplementary Table S1 was correlated with the indicated patient and/or disease characteristics. Student's t-test was used to compare the groups: (a)  $p=0.59$ ; (b)  $p=0.12$ ; (d)  $p=0.33$ ; (g)  $p=0.32$ ; one way ANOVA was used to compare the groups: (c)  $p=0.09$ ; (e)  $p=0.49$  (f)  $p=0.08$ .

### Supplementary Figure S3. Indel efficiency and effect of CXCR4 knock-out with CRISPR-Cas9 in OCI-AML3 cells.

- A Efficiency of indel formation with lentiCRISPRv2-sg2 in OCI-AML3 genomic DNA after puromycin selection was assessed with TIDE. The percentage of aberrant sequences achieved with sg2 compared to lentiCRISPRv2-empty vector (control) is shown.
- B Percentages of aberrant sequences before and after the predicted cutting for control and sg2 are shown.
- C *In vitro* growth characteristics of OCI-AML3 cells transduced with control or sg2 after selection with puromycin were determined by counting cells every 24h over 4d.

### Supplementary Figure S4. [<sup>68</sup>Ga]Pentixafor-PET/CT and [<sup>18</sup>F]FDG-PET/CT imaging in a patient with extramedullary relapse of AML.

- A-C [<sup>68</sup>Ga]Pentixafor-PET/MR imaging of patient #5. Trans-axial views of the thorax are shown. The yellow arrows point towards the histologically proven extramedullary relapse.

- A [68Ga]Pentixafor-PET image.
- B MR image.
- C PET/MR fusion.
- D-F [18F]FDG-PET/CT imaging. Trans-axial views of the thorax are shown. The yellow arrows point towards the histologically proven extramedullary relapse.
- D [18F]FDG-PET.
- E Low-dose CT.
- F PET/CT fusion.

**Supplementary Table S1. Patient characteristics CXCR4 expression cohort.**

**Supplementary Table S2. SUV of visually positive or negative AML patients and control patients.**

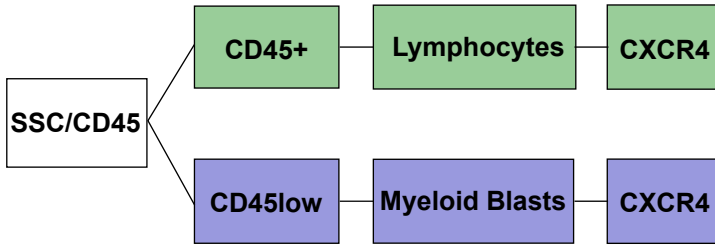
The Table shows the SUV values of all AML patients (#1 - #10) and controls (#11 - #15) measured at the locations indicated in column 1: 1 = cervical vertebra 7; 2 = thoracic vertebra 12; 3 = right os ilium; 4 = lumbal vertebra 5; 5 = left os ilium.

**Supplementary Table S3. Characteristics of the [68Ga]Pentixafor-PET patient imaging cohort.**

Abbreviations: ELN (european leukemia network), fav (favorable), int-1 (intermediate-1), int-2 (intermediate-2), adv (adverse), n.a. (not applicable), MDS (myelodysplastic syndrome), sAML (secondary AML)

Figure S1

A



B

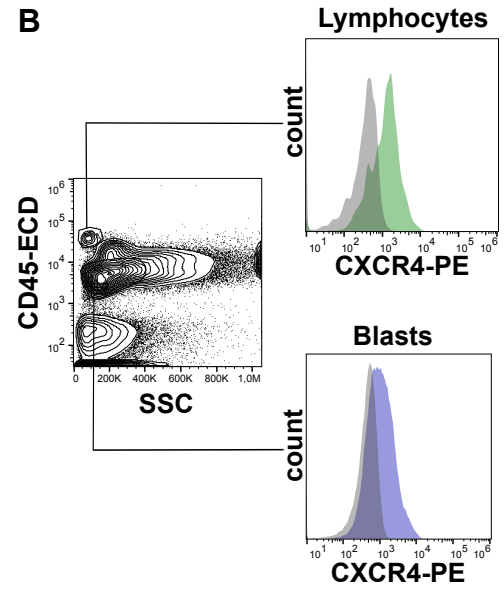


Figure S2

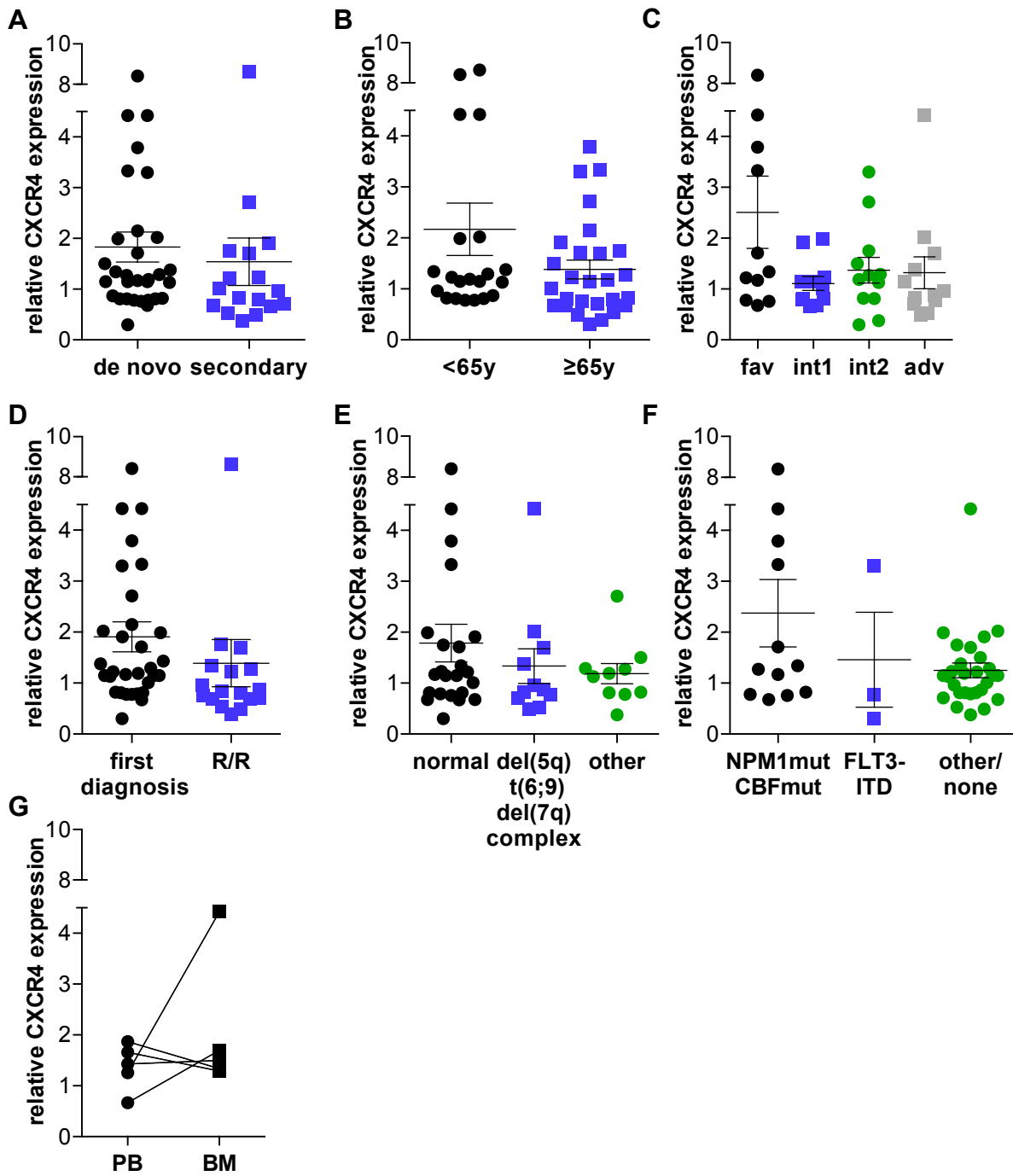
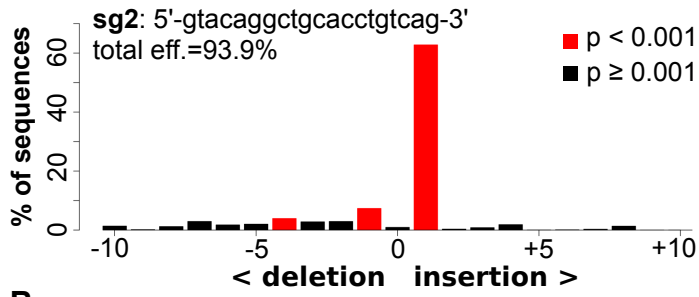
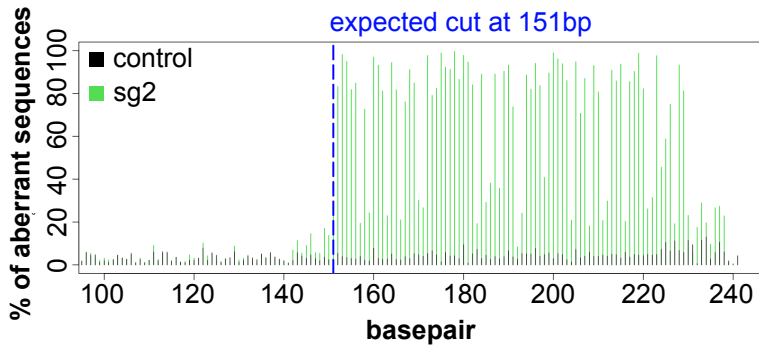


Figure S3

A



B



C

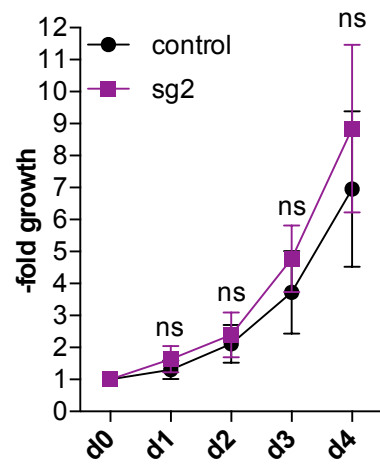
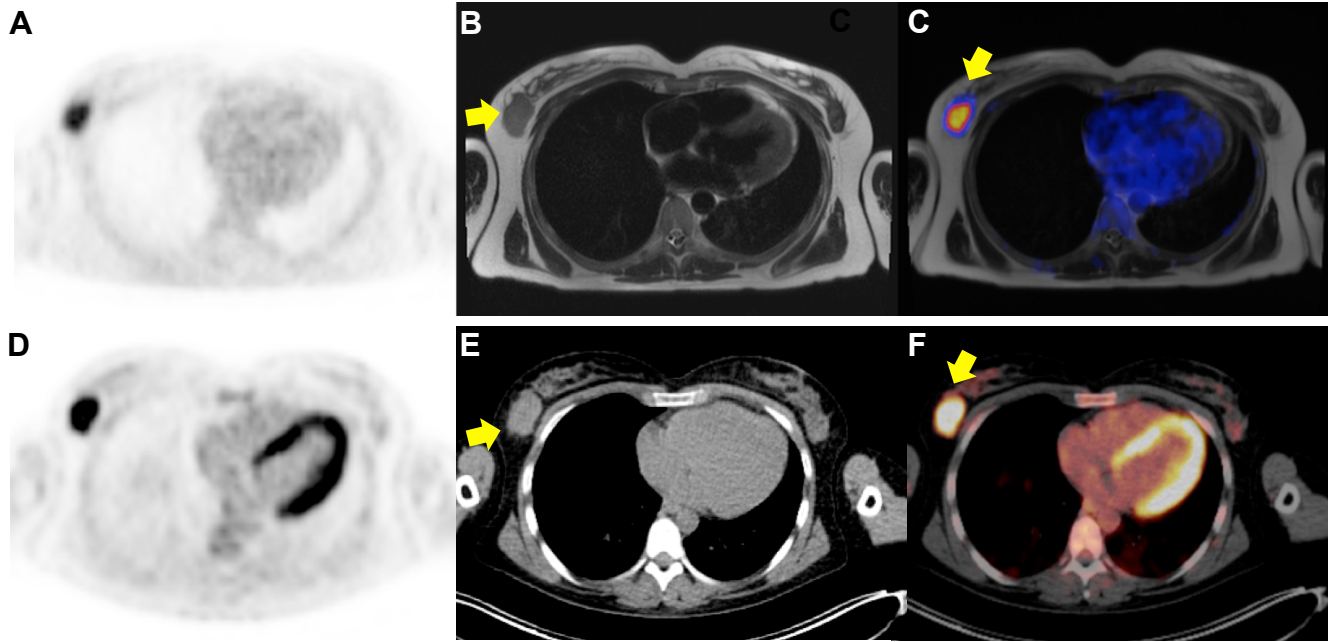


Figure S4



**Supplementary Table S1.** Patient characteristics of the CXCR4 expression cohort

<b>Number of patients</b>	67
<b>Age; years (range)</b>	66 (37-84)
<b>Sex</b>	
male	37/67 (55.2%)
female	30/67 (44.8%)
<b>AML</b>	48/67 (71.6%)
denovo AML	31/48 (64.6%)
secondary AML	17/48 (35.4%)
refractory/relapse disease	17/48 (35.4%)
risk group at diagnosis (ELN)	
favourable	11/48 (22.9%)
intermediate-1	13/48 (27.1%)
intermediate-2	10/48 (20.8%)
adverse	11/48 (22.9%)
not applicable	3/48 (6.3%)
molecular aberrations	
FLT3-ITD	3/48 (6.3%)
NPM1 mut	11/48 (22.9%)
CBF mut	1/48 (2.1%)
none of above aberrations	33/48 (68.8%)
cytogenetic aberrations	
normal KT	23/48 (47.9%)
del(5q); t(6;9); -7; complex KT	11/48 (22.9%)
other aberrations	10/48 (20.8%)
not determined	4/48 (8.4%)
<b>MDS</b>	19/67 (28.4%)
RCMD	8/19 (42.1%)
RAEB-1	6/19 (31.6%)
RAEB-2	5/19 (26.3%)

**Supplementary Table S2.** SUVmax of visually positive or negative AML patients and control patients.

SUVmax															
AML											control				
visually positive						visually negative									
	1	2	3	4	5	6	7	8	9	10	1	2	3	4	5
1	8.1	5.2	4.5	17.1	2.4	2.6	2.1	2.2	2.1	3.3	3.8	2.3	3.2	2.7	2.1
2	10.7	5.8	6.8	15.9	2.6	2.9	2.2	3.1	5.2	3.6	4.5	2.0	2.9	2.7	4.9
3	5.3	3.9	3.1	13.3	0.9	1.5	0.5	1.2	1.1	1.6	1.6	1.4	1.3	1.3	1.3
4	11.7	4.8	5.4	19.8	1.9	2.2	2.8	3.1	3.7	3.9	4.1	2.0	1.8	2.3	3.9
5	4.7	3.5	2.9	12.3	1.3	1.4	0.5	1.1	1.0	1.7	1.7	1.1	1.6	1.2	2.1

SUVmax was measured as indicated in column 1: 1= cervical vertebra 7, 2= thoracic vertebra 12, 3= right os ilium, 4= lumbal vertebra 5, 5= left os ilium

**Supplementary Table S3.** Characteristics of the [68Ga]Pentixafor-PET patient imaging cohort.

patient	age	sex	diagnosis	cytogenetics	molecular aberrations	risk group (ELN)	disease stage	therapy line before imaging
1	72	female	AML FAB M1	46, XY	NPM1 mut	fav		0
2	76	male	sAML	46, XY	NPM1mut; FLT3-TKD+	fav	refractory	2
3	69	male	sAML	45, XY, -7	c-KITD816V mut; CSF3R mut; JAK2 mut; U2AF1 mut	adv	progress	1
4	75	male	AML FAB M5b	46, XY	NPM1 mut	fav		0
5	31	female	AMLFAB M4eo t(16;16)(p13;q22)	46, XX,	CBFB/MYH1 1-rearrangement	fav	extra-medullary relapse after allogeneic PBSCT	2
6	80	male	MDS RAEB 2	46, XY	ASXL1 mut; RUNX1 mut	n.a.	refractory	1
7	57	female	AML FAB M5a	46, XX	none	int-1	refractory	3
8	76	male	sAML	46, XY	NPM1 mut; FLT3-TKD+	fav	refractory	2
9	55	male	AML FAB M1	46, XY	none	int-1		0
10	59	male	AML FAB M1	46, XY	NPM1 mut	fav	refractory	1

Abbreviations: ELN (european leukemia network), fav (favorable), int-1 (intermediate-1), int-2 (intermediate-2), adv (adverse), n.a. (not applicable), MDS (myelodysplastic syndrome), sAML (secondary AML)